

1 **A collaborative online AI engine for CT-based COVID-19 diagnosis**

2
3 Yongchao Xu^{1,2#}, Liya Ma^{1#}, Fan Yang^{3#}, Yanyan Chen^{4#}, Ke Ma², Jiehua Yang², Xian Yang², Yaobing
4 Chen⁵, Chang Shu², Ziwei Fan², Jiefeng Gan², Xinyu Zou², Renhao Huang², Changzheng Zhang⁶,
5 Xiaowu Liu⁶, Dandan Tu⁶, Chuou Xu¹, Wenqing Zhang², Dehua Yang⁷, Ming-Wei Wang⁷, Xi Wang⁸,
6 Xiaoliang Xie⁸, Hongxiang Leng⁹, Nagaraj Holalkere¹⁰, Neil J. Halin¹⁰, Ihab Roushdy Kamel¹¹, Jia Wu¹²,
7 Xuehua Peng¹³, Xiang Wang¹⁴, Jianbo Shao¹³, Pattanasak Mongkolwat¹⁵, Jianjun Zhang^{16,17}, Daniel L.
8 Rubin¹⁸, Guoping Wang⁵, Chuangsheng Zheng^{3*}, Zhen Li^{1*}, Xiang Bai^{2*}, Tian Xia^{2,5*}

9 ¹Department of Radiology, Tongji Hospital, Tongji Medical College, Huazhong University of Science and
10 Technology, Wuhan 430030, China.

11 ²School of Electronic Information and Communications, Huazhong University of Science and Technology, Wuhan
12 430074, China.

13 ³Department of Radiology, Union Hospital of Tongji Medical College, Huazhong University of Science and
14 Technology, Wuhan 430022, China.

15 ⁴Department of Information Management, Tongji Hospital, Huazhong University of Science and Technology,
16 Wuhan 430030, China.

17 ⁵Institute of Pathology, Tongji Hospital, Tongji Medical College, Huazhong University of Science and Technology,
18 Wuhan 430030, China.

19 ⁶HUST-HW Joint Innovation Lab, Wuhan 430074, China.

20 ⁷The National Center for Drug Screening, Shanghai Institute of Materia Medica, Chinese Academy of Sciences,
21 Shanghai 201203, China.

22 ⁸CalmCar Vision System Ltd., Suzhou, China.

23 ⁹SAIC Advanced Technology Department, SAIC, Shanghai, China.

24 ¹⁰CardioVascular and Interventional Radiology, Radiology for Quality and Operations, The CardioVascular Center
25 at Tufts Medical Center, Radiology, Tufts University School of Medicine.

26 ¹¹Russell H Morgan Department of Radiology & Radiologic Science, Johns Hopkins hospital, Johns Hopkins
27 Medicine Institute, 600 N Wolfe St, Baltimore, MD 21205 USA.

28 ¹²Department of Radiation Oncology, Stanford University School of Medicine, 1070 Arastradero Rd, Palo Alto,
29 CA94304.

30 ¹³Department of Radiology, Wuhan Children's Hospital, Wuhan, China.

31 ¹⁴Department of Radiology, Wuhan Central Hospital, Wuhan, China.

32 ¹⁵Faculty of Information and Communication Technology, Mahidol University, Thailand.

33 ¹⁶Thoracic/Head and Neck Medical Oncology, ¹⁷Translational Molecular Pathology, The University of Texas MD
34 Anderson Cancer Center, Houston, Texas 77030, USA.

35 ¹⁸Department of Biomedical Data Science, Radiology and Medicine, Stanford University, USA.

36
37 #These authors contributed equally to this work.

38 *Correspondence should be addressed to T.X. (tianxia@hust.edu.cn), X.B. (xbai@hust.edu.cn),
39 Z.L. (zhenli@hust.edu.cn), or C.Z. (hqzcsx@sina.com).

40

41 **Abstract**

42 Artificial intelligence can potentially provide a substantial role in streamlining chest computed
43 tomography (CT) diagnosis of COVID-19 patients. However, several critical hurdles have
44 impeded the development of robust AI model, which include deficiency, isolation, and
45 heterogeneity of CT data generated from diverse institutions. These bring about lack of
46 generalization of AI model and therefore prevent it from applications in clinical practices. To
47 overcome this, we proposed a federated learning-based Unified CT-COVID AI Diagnostic
48 Initiative (UCADI, <http://www.ai-ct-covid.team/>), a decentralized architecture where the AI
49 model is distributed to and executed at each host institution with the data sources or client ends
50 for training and inferencing without sharing individual patient data. Specifically, we firstly
51 developed an initial AI CT model based on data collected from three Tongji hospitals in Wuhan.
52 After model evaluation, we found that the initial model can identify COVID from Tongji CT test
53 data at near radiologist-level (97.5% sensitivity) but performed worse when it was tested on
54 COVID cases from Wuhan Union Hospital (72% sensitivity), indicating a lack of model
55 generalization. Next, we used the publicly available UCADI framework to build a federated
56 model which integrated COVID CT cases from the Tongji hospitals and Wuhan Union hospital
57 (WU) without transferring the WU data. The federated model not only performed similarly on
58 Tongji test data but improved the detection sensitivity (98%) on WU test cases. The UCADI
59 framework will allow participants worldwide to use and contribute to the model, to deliver a
60 real-world, globally built and validated clinic CT-COVID AI tool. This effort directly supports
61 the United Nations Sustainable Development Goals' number 3, Good Health and Well-Being,
62 and allows sharing and transferring of knowledge to fight this devastating disease around the
63 world.

64 **Introduction**

65 COVID-19 has become a global pandemic. RT-PCR was adopted as the main diagnostic
66 modality to detect viral nucleotide in specimens from patients with suspected COVID-19
67 infection and remained as the gold standard for active disease confirmation. However, due to the
68 greatly variable disease course in different patients, the detection sensitivity is only 60%-71%¹⁻³
69 leading to considerable false negative results. These symptomatic COVID 19 patients and
70 asymptomatic carriers with false negative RT-PCR results pose a significant public threat to the
71 community as they may be contagious. As such, clinicians and researchers have made
72 tremendous efforts searching for alternative and/or complementary modalities to improve the
73 diagnostic accuracy for COVID-19.

74 COVID-19 patients present with certain unique radiological features on chest computed
75 tomography (CT) scans including ground glass opacity, interlobular septal thickening,
76 consolidation etc., that have been used to differentiate COVID-19 from other bacterial or viral
77 pneumonia or healthy individuals⁴⁻⁷. CT has been utilized for diagnosis of COVID-19 in some
78 countries and regions with reportedly sensitivity of 56-98%^{2,3}. However, these radiologic
79 features are not specifically tied to COVID-19 pneumonia and the diagnostic accuracy heavily
80 depending on radiologists' experience. Particularly, insufficient empirical understanding of the
81 radiological morphology characteristic of this unknown pneumonia resulted in inconsistent
82 sensitivity and specificity by varying radiologists in identifying and assessing COVID-19. A
83 recent study has reported substantial differences in the specificity in differentiation of COVID-19
84 from other viral pneumonia by different radiologists⁸. Meanwhile, CT-based diagnostic
85 approaches have led to substantial challenges as many suspected cases will eventually need

86 laboratory confirmation. Therefore, there is an imperative demand for an accurate and specific
87 intelligent automatic method to help to address the clinical deficiency in current CT approaches.
88 Successful development of an automatic method depends on a tremendous amount of imaging
89 data with high quality clinical annotation for training an artificial intelligence (AI) model. We
90 confronted several challenges for developing a robust and universal AI tool for precise COVID-
91 19 diagnosis: 1) data deficiency. Our high-quality CT data sets were only a small sampling of the
92 full infected cohorts and therefore it is unlikely we captured the full set radiological features. 2)
93 data isolation, Data derived across multiple centers was difficult to transfer for training due to
94 security, privacy, and data size concerns. and 3) data heterogeneity. Datasets were generated by
95 different scanner machines which introduces an additional layer of complexity to the training
96 because every vendor provides some unique capabilities. Furthermore, it is unknown whether
97 COVID-19 patients in diverse geographic locations, ethnic groups, or demographics show
98 similar or distinct CT image patterns. All of these may contribute to a lack of generalization for
99 an AI model, which a serious issue for a global AI clinical solution.

100 To solve this problem, we propose here a Unified CT-COVID AI Diagnostic Initiative (UCADI)
101 to deliver an AI-based CT diagnostic tool. We base our developmental philosophy on the
102 concept of federated learning, which enables machine learning engineers and medical data
103 scientists to work seamlessly and collectively with decentralized CT data without sharing
104 individual patient data, and therefore every participating institution can contribute to AI training
105 results of CT-COVID studies to a continuously-evolved and improved central AI model and help
106 to provide people worldwide an effective AI model for precise CT-COVID diagnosis (Fig.1).

107

108 **Results**

109 **Building AI model using pooled data**

110 We firstly gathered a dataset of 5732 CT images from 1276 individuals collected from multiple
111 centers of Tongji Hospital including Tongji Hospital Main Campus (3457 CT images from 800
112 studies), Tongji Optical Valley Hospital (882 CT images from 227 studies), and Tongji Sino-
113 French New City Hospital (1393 CT images from 241 studies) (Table 1 for patient information).
114 Among these patients, 432 patients had COVID-19 pneumonia confirmed by RT-PCR; 76
115 patients had other viral pneumonia including 7 cases with respiratory syncytial virus (RSV), 13
116 with EB virus, 16 with cytomegalovirus, 3 with influenza A, 1 with parainfluenza virus and 36
117 with mixed virus pneumonia that were confirmed PCR or antibodies against corresponding
118 viruses; 350 patients had bacterial pneumonia confirmed CT scan and bacterial culture. The
119 remaining 418 individuals having clinical symptoms of respiratory system were healthy
120 individuals who had normal chest CT scans. Based on the dataset, we developed an initial deep
121 learning model by using convolutional neural networks (CNN) (detailed in Methods).
122 Next, we validated the predictive performance of the CNN through a classification task: four-
123 class pneumonia partition—four featured clinical diagnoses in determining suspected cases of
124 COVID-19. This task aimed at distinguishing COVID-19 (Fig. 3. i) from three types of non-
125 COVID-19 (Fig. 3. ii) including other viral pneumonia, bacterial pneumonia, and healthy cases
126 (d, e, and f in Fig. 3). We selected 20% of 1036 CT cases in training and validation set for 5-fold
127 cross-validation. The CNN demonstrated the validation result that achieved overall sensitivity of
128 77.2% and specificity of 91.9%.

129 We further tested the previously trained CNN by conducting a comparative study of same task
130 between the CNN and expert radiologists using previously separated test set (detailed in
131 Methods). Six qualified radiologists (ZL [18 years' experience], LYM [9 years' experience],
132 YZL [9 years' experience], COX [8 years' experience], HLM [4 years' experience], GC [4
133 years' experience]) from department of radiology, Tongji Hospital (Main campus), Wuhan,
134 China were asked to make diagnosis as one of above 4 classes based on CT study. In this task,
135 the CNN achieved a sensitivity of 97.5% and specificity of 89.4% in differentiating COVID-19
136 from three types of non-COVID-19 cases whereas six radiologists obtained the average 79% in
137 sensitivity (87.5%, 90%, 55%, 80%, 68%, 93%, respectively, and 90% for the maximal voting
138 value among six radiologists), and 90% in specificity (92%, 97%, 89%, 95%, 88%, 79%,
139 respectively, and 95.6% for the maximal voting value) (Fig 4). In the Tongji dataset, the CNN
140 shows performance approaching that of expert radiologists. To examine the reliability of the
141 model, we performed class activation mapping (CAM) analysis for raw CT images in both
142 validation and test datasets⁹ and visualized the featured image regions which lead to
143 classification decision. As shown in Figure 3. iii, the heatmap generated by CAM mostly
144 characterized local lesions suggesting the model learned radiologic features rather than simply
145 overfitting the dataset.

146 To comprehensively evaluate the comparisons of two tasks, we visualized the correlation of
147 sensitivity and specificity via receiver operating characteristic (ROC) curve to calculate the area
148 under the curve (AUC) for representing the CNN's classification performance. As a result, the
149 AUC of the CNN attained 0.98, 0.88, 0.91, 0.98 in specifically identifying COVID-19 pneumonia,
150 other viral pneumonia, bacterial pneumonia, and healthy tissue from 4 classes, and 0.92, 0.92,
151 0.95 in assessing three ordinal severities of COVID-19. Fig. 4 illustrates the ROC curve of the

152 CNN and sensitivity-specificity points displaying radiologists' diagnosis. Importantly, the CNN
153 performed comparable sensitivity-specificity to all six radiologists in differentiating COVID-19
154 from non-COVID-19 cases (Fig. 4a). Meanwhile, the CNN also performed equivalent
155 sensitivity-specificity in comparison with average radiologists in the assessment of three
156 severities (e, f, g in Fig. 4). However, the CNN revealed insufficient capability in determining
157 other viral pneumonia (Fig. 4b), bacterial pneumonia (Fig. 4c), and healthy case (Fig. 4d).

158 To test the generalization of the initial model that was trained exclusively on data from Tongji
159 hospitals, we evaluated the predictive performance using CT data from 100 confirmed COVID-
160 19 cases generated at Wuhan Union hospital. The accuracy of the model was only 72%,
161 compared with a 97% sensitivity using reserved testing data from Tongji hospitals. This
162 demonstrated a lack of generalization for the initial model.

163 **The global online AI diagnostic engine enabled with federated learning**

164 To overcome the hurdle, we proposed a federated learning framework to facilitate UCADI, a
165 global joint effort to generate an AI based on large scale data and integration of diverse ethnic
166 patient groups. In the traditional AI approach, sensitive user data from different sources are
167 gathered and transferred to a central hub where models are trained and generated. The federated
168 learning proposed by Google¹⁰, in contrast, is a decentralized architecture where the AI model is
169 distributed to and executed at each host institution with the data sources or client ends for
170 training and inferencing. The local copies of the AI model on the host institution eliminate
171 network latencies and costs incurred due to sharing large size of data with the central server.
172 Most importantly, the strategy privacy preserved by design enables medical centers collaborating
173 on the development of models, but without need of directly sharing sensitive clinical data with
174 each other.

175 We implemented the federated learning framework at <http://www.ai-ct-covid.team/> where we
176 deployed the initial model to provide 1) online diagnostic interface allowing people easily query
177 the model with patient CT images and 2) AI development federated learning interface(detailed in
178 Methods). UCADI stakeholders can download the code and train a new model based on the
179 initial model. Once the new model had been trained locally for several iterations, if UCADI
180 participants share their updated version of the model, the framework will encrypt the model
181 parameters based on Learning with Errors (LWE)-based encryption¹¹ and transfer them back to
182 the centralized server via a customized server protocol. Participants' datasets will keep within
183 their own secure infrastructure. The central server would then combine the contributions from all
184 of the UCADI participants. The updated model parameters would then be shared with all
185 participants, which enables continuation of local training. The framework is highly flexible,
186 allowing hospitals join or leave the UCADI initiative at any moments, because it is not tied to
187 any specific data cohorts.

188 With the framework, we deployed two experiments to validate federated learning concept on the
189 CT COVID data. Firstly, we trained three models for each of three Tongji hospital datasets, and
190 then transferred the datasets to three physically independent computer servers, respectively, and
191 trained a Tongji federated model in a simulation mode (detailed in Methods). As shown in Figure
192 4. e-h, the federated model performed close to the centralized-trained initial model and better
193 than Tongji Main Campus model for predicting COVID-19, bacterial pneumonia and healthy
194 case (the comparison not applied to models of Tongji Sino-French Hospital and Tongji Optics
195 Valley because they lack of other viral pneumonia data). It shows the effectiveness of federated
196 model. In the second experiment, we trained a federated model in real mode based on three
197 Tongji hospital datasets (432 COVID-19 cases) and 407 confirmed COVID-19 cases from

198 Wuhan Union hospital. We tested the federated model performance on predicting the same 100
199 confirmed Wuhan Union COVID-19 cases which we used to test the initial model previously.
200 The result, 98% sensitivity, was improved compared to the initial model (72% sensitivity) which
201 was centralized trained only based on data from three Tongji hospitals.

202 **Discussion**

203 COVID-19 is a global pandemic. Over 2 million people have been infected, tens of thousands
204 hospitalized, and nearly 200,000 have died worldwide as of April 23rd, 2020. There are borders
205 between countries. But only real border in this war is the border between human being and virus.
206 We need a global joint effort to fight the virus. The first challenge we have confronted in this
207 war is to deliver is deliver people precise and effective diagnosis. In this study, we introduce a
208 globally collaborative AI initiative framework, UCADI, to assist radiologists, streamline, and
209 accelerate CT-based diagnosis. Firstly, we developed an initial CNN model that achieved a
210 performance comparable to expert radiologist in classifying pneumonia to identify COVID-19,
211 and additionally assessing the severity of identified COVID-19. Furthermore, we developed a
212 federated learning framework, based on which hospitals worldwide can join UCADI to jointly
213 train an AI-CT model for COVID-19 diagnosis. With CT data from multiple Wuhan hospitals,
214 we confirmed the effectiveness of this the federated learning approach. We have shared the
215 initial model and the federated learning programmatic API source code
216 (<https://github.com/HUST-EIC-AI-LAB/>) and encourage hospitals worldwide join UCADI to
217 form an international collaboration to fight the virus with a globally trained AI application. It is
218 worth noting that there is still need for improvement in the technical implementation in the
219 framework: 1) The number of local training iterations before global parameter updating. The
220 number of local training iterations has a direct influence on the training efficiency, effectiveness,

221 and model performance. Currently, different clients in UCADI framework train with their private
222 data for one epoch before sending the parameter gradients to the global server. We will construct
223 more detailed experiments about this hyper-parameter to explore the best trade-off between
224 model performance and communication cost. 2) Private information leakage from gradients.
225 Reconstruction of input data from the parameter gradients is possible for realistic deep
226 architectures, and an encryption-decryption module is needed in the federated learning
227 framework. We have adopted an additively homomorphic encryption scheme in our COVID
228 diagnosis framework. The parameter gradients sent to the global server are encrypted while the
229 secret key is kept confidential from the global server, which guarantees the privacy security of
230 our framework. 3) Non-IID and unbalanced data distribution. The training data available is
231 typically based on the patients in the hospital, and any particular hospital's local dataset will not
232 be representative of the entire distribution. Therefore, it requires a dynamic aggregation method
233 that aggregates different parameter gradients via dynamic weighted averaging. Hence, it can
234 decrease the influence of non-IID and unbalanced data.

235 **Methods**

236 **CT data collecting and processing**

237 This study was approved by the Ethics Committee Tongji Hospital, Tongji Medical College of
238 Huazhong University of Science and Technology to access this dataset for research purpose.
239 Here we list the three major scanners used to obtain CT scans: GE Medical
240 System/LightSpeed16, SOMATOM Definition AS+, and GE Medical Systems/Discovery 750
241 HD. The scanning protocols of slice thicknesses and reconstruction kernel were 1.25mm and
242 adaptive statistical iterative reconstruction (60%) for two GE scanners whilst 1mm and sinogram
243 affirmed iterative reconstruction for the Siemens scanner. The high-quality CT image data from

244 the 432 COVID-19 patients were scanned, enrolled, selected and annotated in this study since
245 January 7, 2020 while other image data were retrospectively collected from CT databases of the
246 three Tongji Hospitals. In addition, we collected an independent cohort including 507 COVID-19
247 pneumonia CT cases confirmed by chest CT from Union Hospital, Wuhan, China. The cohort
248 was used for testing the performance of initial model and the multi-hospital model using
249 federated learning framework.

250 We conducted image processing of the raw CT image data to reduce computing burdens. We
251 utilized a sampling method to select 5 subsets of CT slices from all sequential images of one CT
252 case using random starting positions and scalable sampling intervals on transverse view to
253 picture the infected lung regions. All 5 processed subsets were separately fed to the CNN to
254 obtain average predictive probabilities, which can effectively include impacts of different levels
255 of lung from all CT slices. To further improve computing efficiency, we resized each slice from
256 512 to 128 pixel regarding its width and height and rescaled the lung windows of CT to a range
257 from -1200 to 600 and normalized them via the Z-score means before feeding the CNN.

258 **Building AI model using pooled data**

259 The dataset was split out into the training and validation set with 1036 cases (80% for training,
260 20% for validation), and independent test set with 240 cases consisting of 80 COVID-19 studies
261 (28 from Main Campus Hospital, 30 Sino-French New City Hospital, 20 Optical Valley
262 Hospital), 20 with other viral pneumonia (19 from Main Campus Hospital, 1 Sino-French New
263 City Hospital), 60 with bacterial pneumonia (50 from Main Campus Hospital, 8 Sino-French
264 New City Hospital, 2 Optical Valley Hospital), and 80 healthy cases (58 Main Campus Hospital,
265 10 Sino-French New City Hospital, 12 Optical Valley Hospital). We particularly considered the
266 balanced data distribution of 4 classes in test set. We initially trained a four-class CNN (Fig. 2)

267 based on 3D-Densenet¹², a densely connected convolutional network, which performed
268 remarkable advantages in classifying CT images. We customized its architecture to contain 14
269 3D-convolution layers distributed in 6 dense blocks and 2 transmit blocks (Fig. 2b indicating the
270 architecture and data flow). The CNN took 16 resized 128-x128-pixel CT image sequences as
271 input of each CT case, and generated a predicted pneumonia type with maximum probability as
272 output across thousands of attached computing neurons. We defined the loss function as the
273 weighted cross entropy between predicted probability and the true labels. Fine-tuned parameters
274 of the network via back-propagation were optimized using batch size of 16, learning rate of 0.01,
275 weight decay of 0.0001, momentum of 0.9, and epsilon of 0.00001. We conducted the training
276 process utilizing a workstation equipped with 2 Tesla V100 GPUs, costing 6 hours to finish the
277 task.

278 **Building AI model using federated learning**

279 Data preparation:

280 In experiment I, we trained with data collected from multiple centers of Tongji Hospital
281 including Tongji Hospital Main Campus, Tongji Optical Valley Hospital, and Tongji Sino-
282 French New City Hospital. We assigned each hospital to a federated client and place their local
283 data on three different physical machines. In experiment II, besides data collected from above
284 three hospitals, we added Wuhan Union Hospital as a new participant,

285 Federated model setup:

286 For all experiments, we used the same architecture (3D-Densenet) with data-centralized training
287 and the same set of local training hyperparameters for all clients with SGD optimizer: batch size
288 of 35, learning rate of 0.01, momentum of 0.9 and weight decay of 5e-4. In experiment I, we set

289 the number of federated rounds to 200 with one local epoch per federated round. A local epoch
290 means each client train with its local data once before sending information to central
291 server(cloud). We conducted the training process utilizing a workstation equipped with 3 Tesla
292 V100 GPUs, costing 16 hours to finish. In experiment II, we set the number of federated rounds
293 to 30 with one local epoch per federated round and start training with the global model coming
294 from experiment I. For all experiments, we use the same evaluation metric with data-centralized
295 training to check that our procedures are working properly. (In experiment II, we need to train 5
296 rounds before the model achieving the same performance with data-centralized training on test
297 data from Wuhan Union Hospital).

298 **Model aggregation:**

299 The server distributes a global model and receives synchronized weight updates (ΔW_k^t) from all
300 clients at each federated round. Due to each client train with one epoch per federated round, so
301 we just average all the weight updates from the client with equal weight and update the global
302 model.

303 **Privacy-preserving setup:**

304 We use a variant of additively homomorphic encryption to achieve privacy-preserving, which
305 called Learning with Errors (LWE)-based encryption. The encryption method allows us to leak
306 no information of participants to the honest-but-curious parameter (cloud) server.

307 **Data Availability** All relevant data used for developing the initial model and federated models
308 during the current study are not publicly available.

309

310 **Model Availability**

311 The online application of AI model is publicly available at <http://www.ai-ct-covid.team/>.
312 The initial model or offline APP is publicly available upon request at tianxia@hust.edu or
313 xbai@hust.edu.cn or through website <http://www.ai-ct-covid.team/>.

314

315 **Federated Learning Framework Availability.** The source code can be accessed at
316 <https://github.com/HUST-EIC-AI-LAB/>.

317

318 **References**

- 319 1. Ai, T., *et al.* Correlation of chest CT and RT-PCR testing in coronavirus disease 2019 (COVID-
320 19) in China: a report of 1014 cases. *Radiology*, 200642 (2020).
- 321 2. Fang, Y., *et al.* Sensitivity of chest CT for COVID-19: comparison to RT-PCR. *Radiology*,
322 200432 (2020).
- 323 3. Kanne, J.P., Little, B.P., Chung, J.H., Elicker, B.M. & Ketai, L.H. Essentials for radiologists on
324 COVID-19: an update—radiology scientific expert panel. (Radiological Society of North
325 America, 2020).
- 326 4. Chung, M., *et al.* CT imaging features of 2019 novel coronavirus (2019-nCoV). *Radiology* **295**,
327 202-207 (2020).
- 328 5. Kanne, J.P. Chest CT findings in 2019 novel coronavirus (2019-nCoV) infections from Wuhan,
329 China: key points for the radiologist. (Radiological Society of North America, 2020).
- 330 6. Shi, H., *et al.* Radiological findings from 81 patients with COVID-19 pneumonia in Wuhan,
331 China: a descriptive study. *The Lancet Infectious Diseases* (2020).
- 332 7. Vaseghi, G., *et al.* Clinical characterization and chest CT findings in laboratory-confirmed
333 COVID-19: a systematic review and meta-analysis. *medRxiv* (2020).

- 334 8. Bai, H.X., *et al.* Performance of radiologists in differentiating COVID-19 from viral pneumonia
335 on chest CT. *Radiology*, 200823 (2020).
- 336 9. Yao, T., Pan, Y., Li, Y., Qiu, Z. & Mei, T. Boosting image captioning with attributes. in
337 *Proceedings of the IEEE International Conference on Computer Vision* 4894-4902 (2017).
- 338 10. McMahan, H.B., Moore, E., Ramage, D. & Hampson, S. Communication-efficient learning of
339 deep networks from decentralized data. *arXiv preprint arXiv:1602.05629* (2016).
- 340 11. Aono, Y., Hayashi, T., Wang, L. & Moriai, S. Privacy-preserving deep learning via additively
341 homomorphic encryption. *IEEE Transactions on Information Forensics and Security* **13**, 1333-
342 1345 (2017).
- 343 12. Huang, G., Liu, Z., Van Der Maaten, L. & Weinberger, K.Q. Densely connected convolutional
344 networks. in *Proceedings of the IEEE conference on computer vision and pattern recognition*
345 4700-4708 (2017).

346

347 **Acknowledgements**

348 This study was supported by HUST COVID-19 Rapid Response Call (No. 2020kfyXGYJ031,
349 No. 2020kfyXGYJ093, No. 2020kfyXGYJ094) and the National Natural Science Foundation of
350 China (61703171 and 81771801). This work was also supported in part by a grant from the
351 National Cancer Institute, National Institutes of Health, U01CA242879, and Thammasat
352 University Research fund under the NRCT, Contract No. 25/2561, for the project of “Digital
353 platform for sustainable digital economy development”, based on the RUN Digital Cluster
354 collaboration scheme.

355 **Author contributions**

356 T.X., X.B., Z.L., and C.Z., conceived the work. Y.X., L.M., F.Y., K.M., J.Y., X.Y., C.S., Z.F.,
357 J.G., X.Z., R.H., C.Z., X. L., D.T., C.X., W.Z., D.Y., M.W., N.H., N.J.H., I.R.K., X.P., X.W.,

358 J.B. designed and developed the models and analyses; Y.X., K.M., D.L.R., J.Z., and T.X.
359 interpreted results; and K.M., J.W., P.M., D.L.R., J.Z., Z.L., and T.X. wrote the paper.

360 **Competing interests**

361 The authors declare no competing interests.

362

363 **Tables**

	Male	Female	0-20 years	20-40 years	40-60 years	60-80 years	>80 years
Patient Number	617	659	40	444	421	340	31

364 **Table 1** | Patient information of 1276 studies collected from Tongji Hospital regarding gender
365 and age distribution.

366

367

368

369

370

371

372

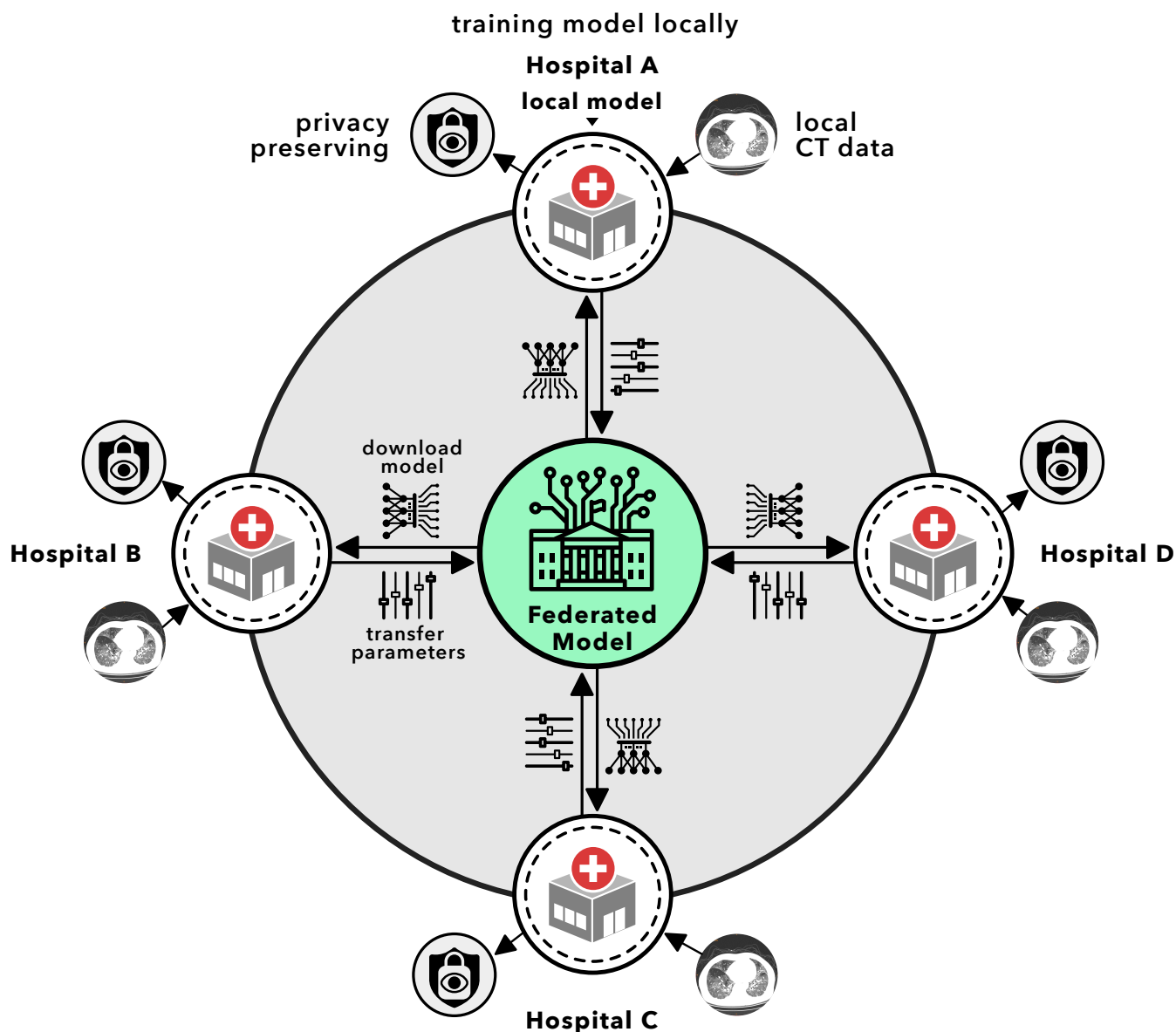


Figure 1 | The conceptual architecture of UCADI on the basis of federated learning. UCADI stakeholders firstly download the code and train a new model locally based on the initial model, and secondly transfer the encrypted model parameters back to the federated model. The central server combines the contributions shared from all of the UCADI participants.

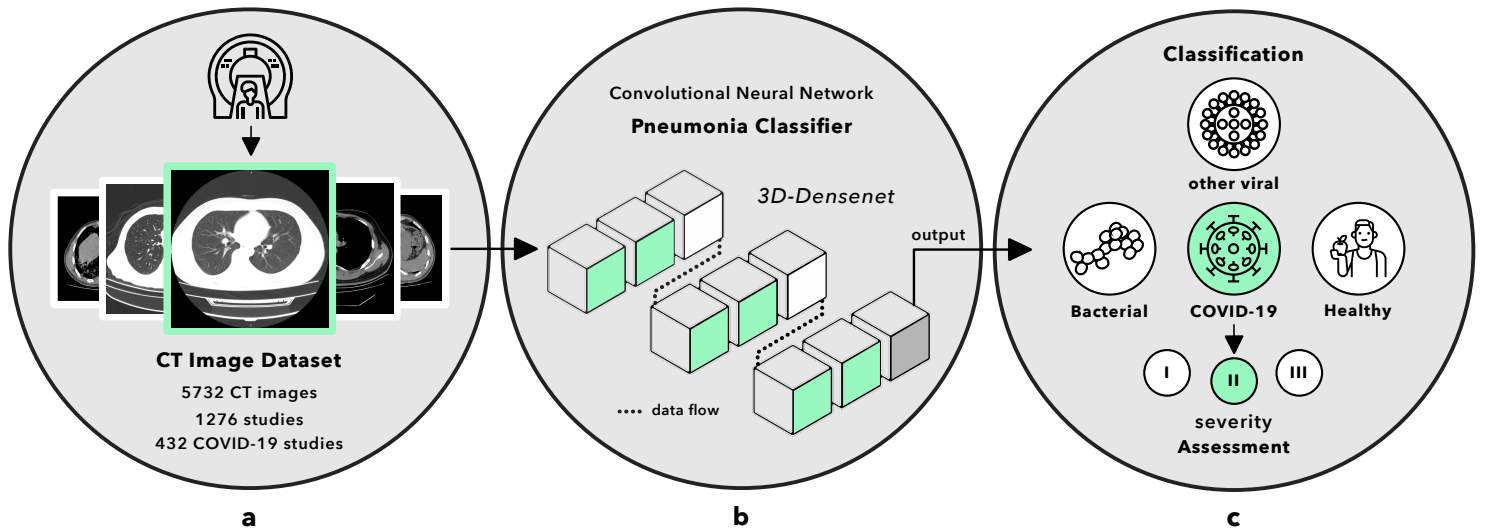
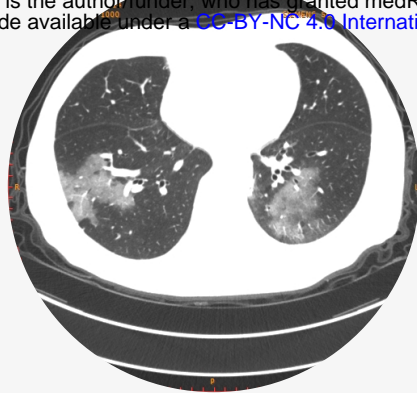


Figure 2 | Data and strategy. **a**, number of CT studies and total images. **b**, the CNN was developed based on 3D-Densenet, consisting of 6 dense blocks in green, 2 transmit blocks in white and an output layer in gray. Pre-processed 128-x-128-pixel CT images of one case were fed to the network across 14 3D-convolution layers and a number of functions embedded in 3D blocks, finally received the predicted classification result. **c**, the CNN classified CT case into 4 types and further assessed the severity into I or II or III if the case was predicted as COVID-19.

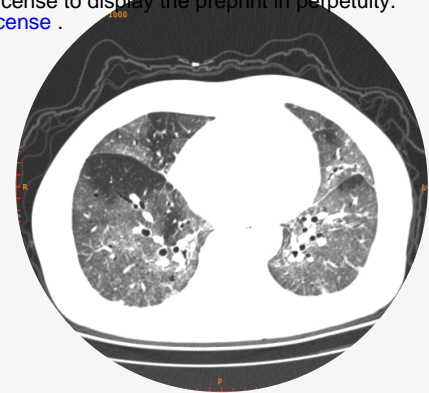
i. medRxiv preprint doi: <https://doi.org/10.1101/2020.05.10.20096073>; this version posted May 19, 2020. The copyright holder for this preprint (which was not certified by peer review) is the author/funder, who has granted medRxiv a license to display the preprint in perpetuity. It is made available under a [CC-BY-NC 4.0 International license](#).



a
COVID-19 pneumonia



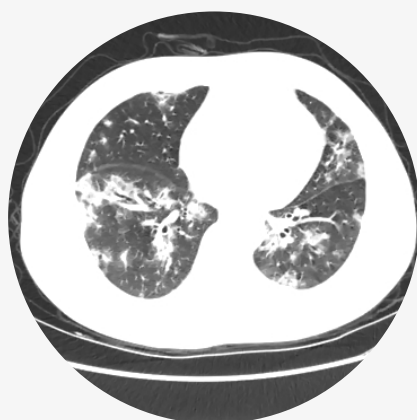
b
COVID-19 pneumonia



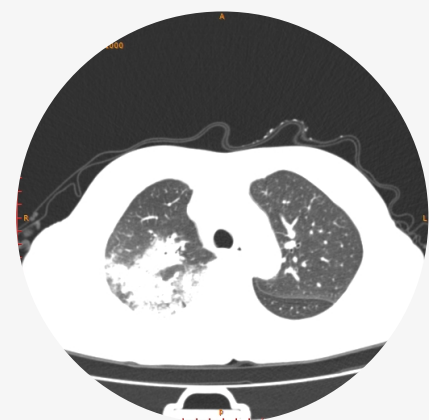
c
COVID-19 pneumonia



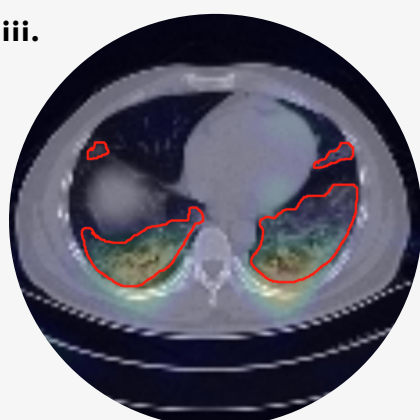
d
healthy



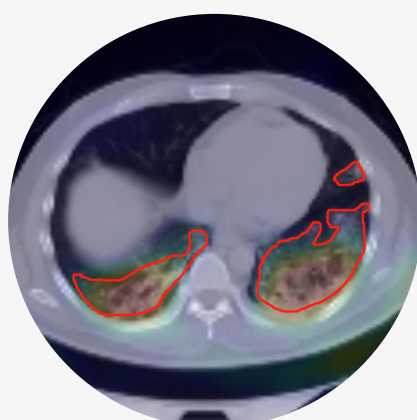
e
other viral pneumonia



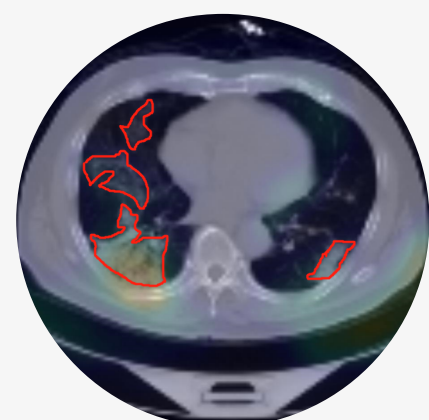
f
bacterial pneumonia



g



h



i

Figure 3 | CT images. i and ii, the taxonomy of pneumonia and featured CT image for per-class. iii, the heatmap generated by GradCAM and local lesions annotated by the radiologist. i, COVID-19 pneumonia. a, b, c represent the CT images of COVID-19 defined by radiological features. ii, non-COVID-19 cases. d, e, f respectively displays the CT image of healthy case, other viral pneumonia, and bacterial pneumonia. iii, CAM visualized the image areas which lead to classification decision. The radiologist, LYM [9 years' experience], from Department of Radiology, Tongji Hospital circumscribed the local lesions with the red curved masks. g-h, patients with COVID-19 pneumonia.

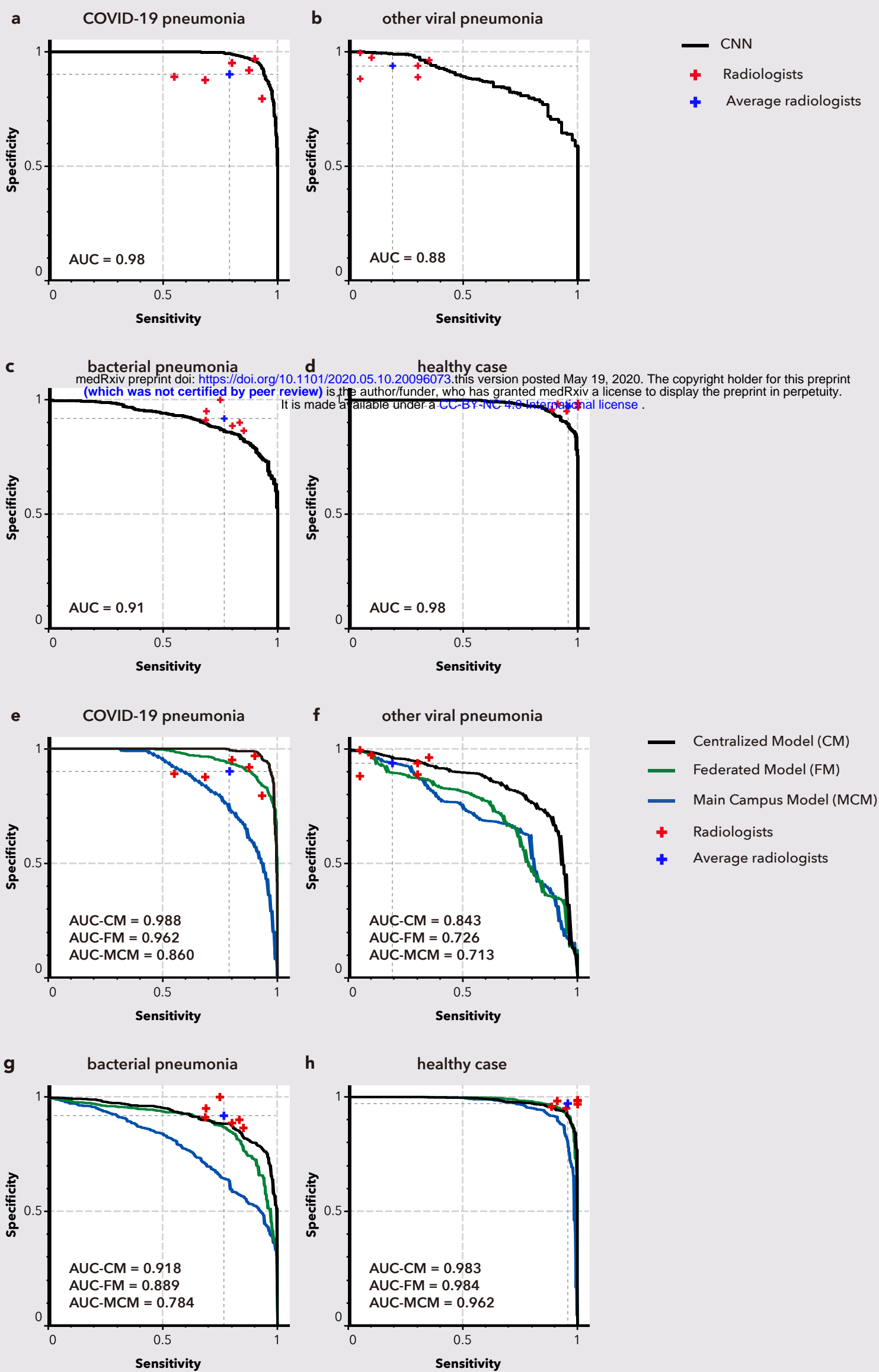


Figure 4 | Pneumonia classification performance of CNN models and radiologists. This figure illustrates the comparative analysis between the CNN and radiologists by correlating the ROC curve of CNN and sensitivity-specificity points of six invited radiologists for two conducted classification test tasks. **a-d**, per-class evaluation for three types of pneumonia and healthy case. The curve in black represents the performance of the CNN. Cross marks in red separately represent the performance of six radiologists and the blue mark annotates the average capability. **e-h**, comparative evaluation of centralized-trained initial model, federated model, and Tongji Main Campus model on four per-class classification tasks.